International Journal of Thermophysics (2022) 43:137
https://doi.org/10.1007/s10765-022-03062-5

Evaluation of Liquid Heat Capacity of Latest Low Global Warming Hydrofluoroolefins (HFOs): A Comparison of a Cubic Equation of State, Fundamental Equations of State, and a Corresponding State Equation

Neng Gao[1,4] · Likai Zhou[2] · Xuehui Wang[3] · Guangming Chen[1,2]

Received: 21 April 2022 / Accepted: 16 June 2022 / Published online: 14 July 2022

Abstract

Isobaric heat capacity is one of the key thermophysical properties for working fluids in thermal systems and plays an important role in the development of equation of state. Due to the lack of experimental data for promising hydrofluoroolefins (HFOs), we carried out theoretical predictions for condensed liquid phase with three different methods: traditional cubic equation of state (CEOS), fundamental equations of state (FEOS) explicit in Helmholtz free energy and a corresponding state equation (CSE). Both CEOS and CSE are generalized models that only need several characteristic parameters to conduct calculation, while FEOS are specific models in which the structure and parameters are regressed from experimental data of one certain fluid. Liquid heat capacity data of 9 HFOs were calculated, including well-known R1234yf, R1234ze(E), and latest prospective R1123, R1216, R1243zf, R1234ze(Z), R1336mzz(Z), R1141, and R1125zc. A critical comparison was carried out between different calculation methods. The comparison showed that both CSE and FEOS predicted available experimental data well with AADs % less than the reported experimental uncertainties. For refrigerants without experimental heat capacity, CSE and FEOS showed good agreements with AADs % less than 3.6 %. The selected CEOS always provided relatively larger predictions than experiments or the other two methods. Despite that, calculated data of CEOS showed a strong linear relation with the other two methods, which suggested that there might be a potential linear modification or correlation for CEOS in improving its heat capacity calculations. Furthermore, when there were no experimental data available, CSE used in this study could be a useful preliminary evaluation tool for the liquid heat capacity of hydrofluoroolefins, considering its accuracy and easy application characteristics.

Keywords Corresponding state equation · Equation of state · HFO refrigerants · Isobaric heat capacity

✉ Xuehui Wang
xwang18@ic.ac.uk

Extended author information available on the last page of the article

1 Introduction

Since the first decade of this century, the whole refrigeration industry has entered a new stage leading by the replacement of refrigerants, the "blood" of refrigerating and air conditioning machines. Due to the increasing challenge of global warming, third-generation refrigerants represented by hydrofluorocarbons (HFCs such as R134a, R410A, and R404A, etc.) have been facing a phase-out situation for their high Global Warming Potential (GWP). Various regional and global protocols and regulations have been put forward over the last twenty years, represented by the European F-gas regulations [1, 2] and the Kigali Amendment [3]. The Kigali Amendment, which came into effect on Jan. 1st, 2019, provides a clear schedule for the phasing-out of high GWP HFCs. therefore, searching and testing new alternative refrigerants became more important and urgent.

Hydrofluoroolefins, the fluoride unsaturated hydrocarbons, are now widely accepted as the most promising alternatives besides natural refrigerants [4]. With unsaturated carbon–carbon bonds, these synthetic compounds have very short expectancy when exposed to the atmosphere, resulting in their ultra-low GWPs [5, 6]. Despite mild flammability, two hydrofluoroolefins (R1234yf and R1234ze(E)) have already been well studied by researchers and introduced into different commercial applications. However, other potential hydrofluoroolefins are not sufficiently understood even in labs at present. Researchers at the National Institute of Standard and Technology (NIST) have carried out a series of work on the screening of potential compounds from all chemical databases [7]. Lists of limited candidates were provided in different application areas and most of them were hydrofluoroolefins.

Thermophysical properties are the foundation of pre-evaluation for alternative refrigerants and performances of their systems. A critical review of thermophysical experimental reports has been contributed recently and shown a lack of data available for HFOs except for R1234yf and R1234ze(E), which largely restrict potential applications [8]. Among various properties, isobaric heat capacity (c_p) is a special one, which associated directly with enthalpy and entropy, making it the basis for thermodynamic calculation and modeling. Meanwhile, as a typical caloric property which is calculated from both 1st and 2nd order derivatives of Helmholtz free energy, c_p also plays an important role in the development of accurate and stable fundamental equations of state.

Flow calorimetry [9], quasi-steady calorimetry [10] and thermal relaxation method [11] can be used to obtain reliable experimental isobaric heat capacity data for liquids under different temperatures and pressures. These methods have already been used on liquid R1234yf and R1234ze(E). However, there are still no experimental data available for other HFOs to our best knowledge. Therefore, theoretical predictions become essential and will be beneficial for researchers and engineers in exploring alternative refrigerants in the current situation.

2 Isobaric Heat Capacity Prediction Methods

The isobaric heat capacity of liquids is split into two parts: an ideal gas term and a residual term. Nowadays, the ideal gas heat capacity is usually obtained by gas sound-speed experiments [12] or vibrational energies [13] and then correlated to a temperature-dependent polynomial function. Alternatively, ideal gas heat capacity can be calculated from *ab* initio or group contributions without experiments [14]. On the other hand, the residual part, which comprises molecular interactions (dispersive and electrostatic interactions) but no contributions from bond stretching, angle bending, and torsion, can be calculated by different theoretical methods.

Theoretical prediction of residual isobaric heat capacity is a representative application of classic thermodynamic relations. It can be performed with different equations of state, such as traditional cubic EOS (CEOS) [15], multi-parameter fundamental EOS (FEOS) [16], perturbation EOS [17] etc. In this study, we selected Peng-Robinson (PR) EOS and Helmholtz free energy EOS. PR EOS is a cubic EOS with volume translation, it has a general expression with only characteristic parameters needed for calculation, and it is predictive among different fluids. Helmholtz free energy EOSs are multi-parameter fundamental EOSs with the highest accuracy in all thermodynamic properties' calculations. Modern FEOSs consist of polynomial, exponential, and Gauss-bell shaped terms. The final structure and coefficients are different for each fluid, which were determined by optimization regression with experimental property data. These FEOSs are predictable for each fluid, which means one can establish a FEOS with for example only vapor pressure and saturated density data, and apply it to calculate other properties such as isobaric heat capacity. It should be noticed that the accuracy of this prediction is not easily guaranteed because 2nd order derivatives are needed in isobaric heat capacity and they are extremely sensitive to the Helmholtz free energy surface.

In recent years, novel EOS such as perturbation EOS (such as PC-SAFT) and cubic plus association EOS (CPA) have also been proposed for alternative refrigerants R1233zd(E), R1234yf, R1234ze(E), and R1234ze(Z) [18]. PC-SAFT is Helmholtz free energy-based and its calculation for isobaric heat capacity follows the same process with FEOS, while CPA is pressure-based, adding an association part to traditional cubic EOS. Both of these EOS have semi-empirical parameters that need to be determined by fitting experimental data. The different fitting strategies would result in different EOS performance. If there were no experimental c_p available in parameter-fitting, the calculation from PC-SAFT and CPA for c_p are unacceptable.

Molecular simulation (MS) is another powerful way to predict the thermodynamic properties of fluids. A series of work on the simulation of the HFOs and their mixtures have been carried out by researchers in the last few years [19–21]. Based on either complicated all-atom force fields or simplified LJ2C force fields, these simulations could provide satisfying results for the volumetric and vapor–liquid equilibrium properties, with several molecular parameters

transferred or correlated by experimental data. However, regarding c_p calculation from molecular simulations, the uncertainty is of the same order of magnitude as the uncertainties for residual configurational energy due to interpolation, which reflects the difficulty of MS in heat capacity calculation [20].

Empirical and semi-empirical methods have also been provided by researchers to predict isobaric heat capacity, such as Group Contribution Method (mostly used for ideal gas heat capacity), Corresponding State Method [22], and data-driven artificial neural network [23]. In this work, a pre-proposed corresponding state equation (CSE) [24] explicit in isobaric heat capacity for hydrofluorocarbons was studied in comparison with selected EOS. The CSE was a four-parameter semi-empirical function with its structure and coefficients correlated from traditional hydrofluorocarbon refrigerants. Since the objects in this study belong to the same class of compounds (short-chain molecules consisting of Hydrogen, Fluorine, and Carbon atoms), they are thought to be more likely to satisfy the assumptions of the corresponding state principle.

The detailed information for the three methods and their calculation form for isobaric heat capacity is listed in Table 1.

3 Comparison and Results

A total of 9 HFOs were investigated in this study and their basic information is shown in Table 2. These HFOs were divided into 3 classes, according to whether they have available experimental data, the fundamental equation of state, and characteristic parameters used in CEOS and CSE.

R1234yf and R1234ze(E) were assigned as Class 1 refrigerants, with experimental c_p data [10, 11, 25, 26] and FEOS reported [27, 28]. Class 2 refrigerants were those who had preliminary FEOS established without experimental c_p, including R1123, R1216, R1234ze(Z), R1243zf, and R1336mzz(Z). Class 3 refrigerants consisted of R1141 and R1225zc, these two HFOs had neither experimental c_p nor FEOS, but only reliable critical points and acentric factors. Other HFOs with only estimated characteristic parameters were not concerned, such as R1132(E), R1234ye(E), R1225ye(Z), R1132(Z), and R1225ye(E).

As shown in Table 1, CEOS and CSE were easily self-programmed, while FEOS used in this study were embedded in the latest version of the NIST Refprop Database [30]. Available information of these FEOSs is listed in Table 3, including their terms and calorimetric properties used in correlation, which is an important factor for evaluating the ability of FEOS in second-order derivative property calculations. Characteristic parameters used for CEOS and CSE were referred to in the recent review [8]. Ideal gas heat capacities were obtained from NIST Refprop Database for class 1 and class 2 refrigerants, and group contribution method for class 3 refrigerants [32]. All the calculation results from CEOS and CSE can be found in the Appendix.

For class 1 refrigerants, calculated liquid c_p data by FEOS, CEOS, and CSE were compared to the experimental reports. As can be seen in Fig. 1, both CSE and FEOS well-presented experimental data of R1234yf and R1234ze(E) in a

Table 1 Description of the models studied in this work

Model type	Research	Model details	Remarks
Peng-Robinson Equation (CEOS)	Peng and Robinson [15]	$p = \frac{RT}{v-b} - \frac{a}{v(v+b)+b(v-b)}$ $a = 0.45724\alpha R^2 T_c^2/p_c, b = 0.07780RT_c/p_c$ $\alpha = [1 + k(1 - T_r^{0.5})]^2 k = 0.37464 + 1.54226\omega - 0.26992\omega^2$ $A = \alpha p/(R^2T^2) B = bp/(RT)$ $C_p - C_p^0 = \alpha'' \frac{T}{2\sqrt{2}b} \ln\left\{\frac{Z + (\sqrt{2}+1)B}{Z - (\sqrt{2}-1)B}\right\} + \frac{R(M-N)^2}{M^2 - 2A(Z+B)} - R$ $M = (Z^2 + 2BZ - B^2)/(Z - B)N = \alpha' B/(bR)$	General model, wide application in industrial clusters in certain process
Helmholtz Equation of State (FEOS)[a]	Schmidt and Wagner [16]	$\frac{a^r(T,\rho)}{\rho RT} = a^r(\tau,\delta) = \sum_{i=1}^{13} n_i \tau^{t_i} \delta^{d_i} + \sum_{i=14}^{24} n_i \tau^{t_i} \delta^{d_i} \exp\left(-\delta^2\right) + \sum_{i=25}^{32} n_i \tau^{t_i} \delta^{d_i} \exp\left(-\delta^4\right)$ $\frac{C_p}{R} = -\tau^2\left[\left(\frac{\partial^2 a^0}{\partial\tau^2}\right)_\delta + \left(\frac{\partial^2 a^r}{\partial\tau^2}\right)_\delta\right] + \frac{\left[1 + \delta\left(\frac{\partial a^r}{\partial\tau}\right)_\delta - \delta\tau\left(\frac{\partial^2 a^r}{\partial\delta\partial\tau}\right)\right]^2}{\left[1 + 2\delta\left(\frac{\partial a^r}{\partial\delta}\right)_\tau + \delta^2\left(\frac{\partial^2 a^r}{\partial\delta^2}\right)_\tau\right]}$	exclusive models, highly accurate, wide range
Corresponding State Equation (CSE)	Gao et al. [24]	$(C_p - C_p^0)/R = [1 + a_0(p_c/p_c^r)\omega + a_1(p_c/p_c^r)\omega^2]\phi(p_r, T_r)$ $\phi(p_r, T_r) = B(T_r) + C(T_r)p_r + D(T_r)p_r^{0.5}$ $B(T_r) = b_0 + b_1(1 - T_r)^{0.5} + b_2(1 - T_r)^{-0.5}$ $C(T_r) = c_0(1 - T_r)^2 + c_1(1 - T_r)^{-1} + c_2(1 - T_r)^{-3.5} + c_3 e^{-(1-T_r)}$ $D(T_r) = d_0(1 - T_r)^{0.5} + d_1(1 - T_r)^2 + d_2(1 - T_r)^3 + d_3(1 - T_r)^{3.5} + d_4(1 - T_r)^{-1}$	General model; Explicit in c_p

[a]Taking the Schmidt and Wagner Equation [16] as an example, which was the first ground-breaking FEOS with a general formula

Table 2 Information table for HFO refrigerants

ASHRAE	IUPAC name	*Tc*/K	*Pc*/MPa	ω	GWP_{100y}	FEOS[a]	EXP.[b]
Class 1							
R1234yf	2,3,3,3-Tetrafluoropropene	367.9	3.38	0.276	< 1	√	√
R1234ze(E)	Trans-1,3,3,3-tetrafluoropropene	382.5	3.64	0.313	6	√	√
Class 2							
R1123	Trifluoroethene	331.7	4.55	0.243	3	√	-
R1216	Hexafluoropropene	358.9	3.15	0.333	0.86	√	-
R1234ze(Z)	1,3,3,3-Tetrafluoroprop-1-ene	423.3	3.53	0.3274	1.4	√	–
R1243zf	3,3,3-Trifluoroprop-1-ene	376.9	3.52	0.2606	0.8	√	–
R1336mzz(Z)	Cis -1,1,1,4,4,4-hexafluoro-2-butene	444.5	2.90	0.3867	2	√	–
Class 3							
R1141	Fluoroethene	327.2	5.16	0.1675	< 1	–	–
R1225zc	1,1,3,3,3-Pentafluoroprop-1-ene	376.6	3.31	0.303	N.A	–	–

[a]FEOS: Fundamental Equation of State available in the latest version of REFPROP[30]

[b]Exp.: Experimental data available in open literatures

Table 3 FEOS information for Class 1 & 2 refrigerants

Name	Terms in EOS[a]	Claimed Uncertainty in Liquid c_p	Caloric properties used in Correlation
R1234yf [27]	15	5 %	*w* [b]
R1234ze(E) [28]	14	5 %	None
R1123 [29]	17	N.A. [c]	*w*
R1216 [30]	16	N.A	N.A
R1234ze(Z) [31]	16	N.A	*w*
R1243zf [31]	15	N.A	None
R1336mzz(Z) [30]	18	N.A	N.A

[a]Terms in the residual part of Helmholtz free energy; [b]Sound of speed; [c]Not available

wide range. The average absolute deviation (AAD %) and maximum absolute deviation (MAD %) between CSE and experimental data were 0.9 % and 4.0 % for R1234yf, and 1.0 % and 3.6 % for R1234ze(E), as listed in Table 4. AAD % and MAD % between FEOS and experimental data were 0.6 % and 3.3 % for R1234yf, and 1.1 % and 4.7 % for R1234ze(E). However, CEOS generally provided calculated values with positive deviations, and the deviations tended to be larger at higher temperatures where the absolute value of c_p became larger. The AAD % and MAD % of CEOS were 6.2 % and 15.6 % for R1234yf, and 4.4 % and 18.4 % for R1234ze(E). An interesting phenomenon is that, despite unacceptable deviations, predicted values of CEOS nearly followed a strong linear relationship to the real values, seen in Fig. 1. The Pearson factor between CEOS calculations

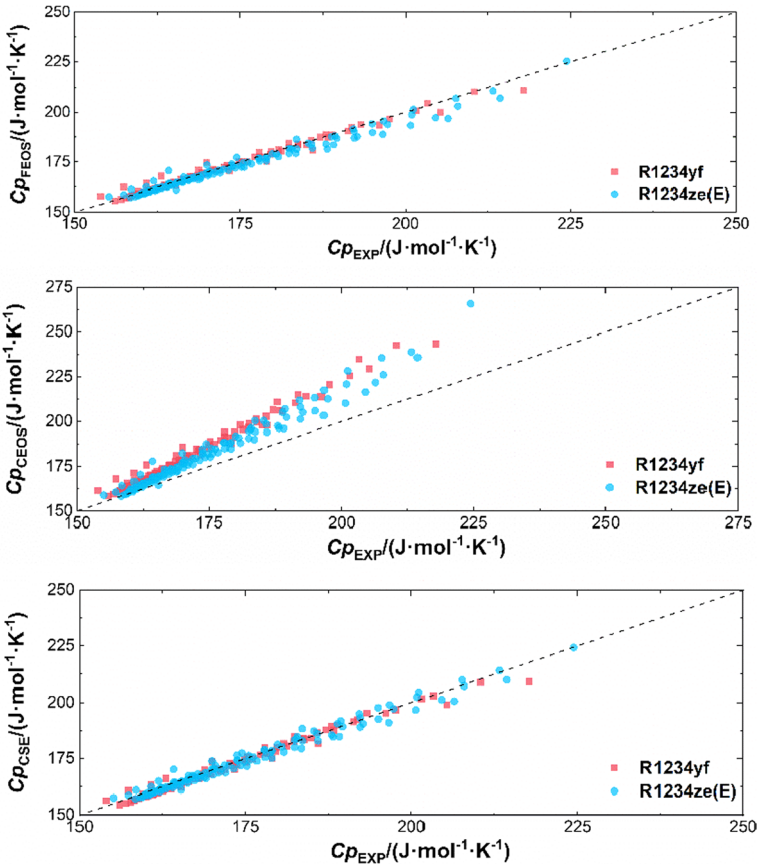

Fig. 1 Comparison between calculated liquid heat capacity for *Class 1* refrigerants by FEOS, CEOS and CSE

Table 4 Comparison between predictions and experimental data for Class 1 refrigerants

Name	*T*/K	*P*/MPa	Exp. Uncertainty	CSE		FEOS		CEOS	
				AAD %	MAD %	AAD %	MAD %	AAD %	MAD %
R1234yf	305–350	1.5–5.1	1.7 % [9], 5 % [25]	0.9	4.0	0.6	3.3	6.2	15.6
R1234ze(E)	310–365	1.6–5.5	5 % [10], 2.1 % [24]	1.0	3.6	1.1	4.7	4.4	18.4

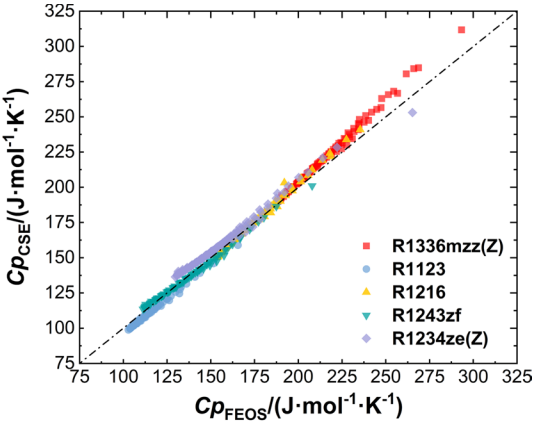

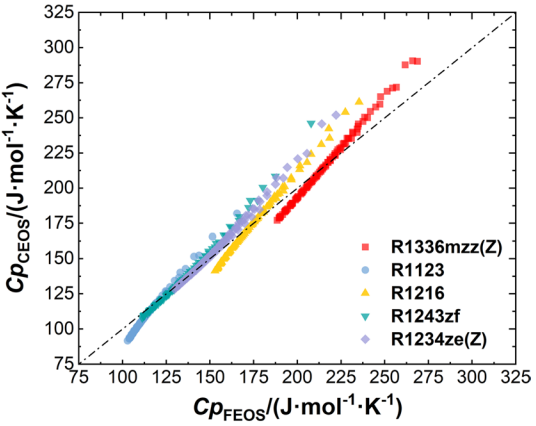

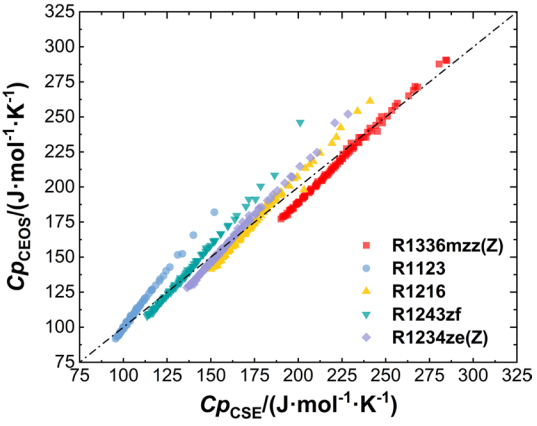

Fig. 2 Cross comparison of liquid heat capacities predicted by CSE, FEOS and CEOS for *Class 2* refrigerants

Table 5 Cross comparison between CEOS, FEOS and CSE for Class 2 refrigerants[a]

Name	T/K	CSE VS FEOS		CEOS VS CSE		CEOS VS FEOS	
		AAD %	MAD %	AAD %	MAD %	AAD %	AAD %
R1123	210–320	3.6	5.6	4.4	14.5	5.3	10.8
R1216	210–350	0.9	5.9	3.3	8.7	3.8	11.7
R1234ze(Z)	250–410	3.2	6.8	3.7	32.9	3.0	26.9
R1243zf	220–360	1.3	3.9	4.0	22.4	2.7	18.4
R1336mzz(Z)	270–430	2.7	7.2	3.3	7.1	3.2	12.8

[a]Pressures range from 1 to 10 MPa

and experimental data were 0.9925 for R1234yf and 0.9826 for R1234ze(E), respectively.

For class 2 refrigerants, cross-comparisons between the theoretical methods were performed, with no available experiments. The testing temperature range was set as 210 K to 430 K (different for each one) and pressure range 1 MPa to 10 MPa, respectively. Comparison results are shown in Fig. 2 and Table 5. CSE and FEOS showed very good agreements for class 2 refrigerants with all the AADs % less than 3.6 %, and MADs % less than 7.2 %. Larger deviations trended to occur at higher temperatures. The pair plot between CEOS and FEOS showed similar trends to that between CEOS and CSE. Average deviations between CEOS and CSE were less than 5.1 %, and also a strong linear relationship could be detected for all class 2 refrigerants.

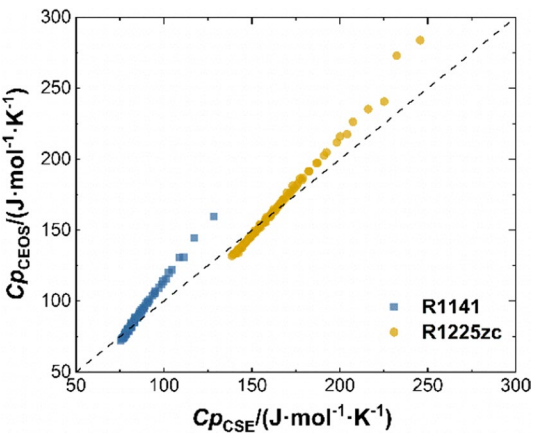

Fig. 3 Comparison of predicted heat capacities for *Class 3* refrigerants by CSE and CEOS

Table 6 Comparison between CEOS and CSE for Class 3 refrigerants

Name	T/K	P/MPa	AAD %	MAD %
R1141	207–316	1.13–11.36	6.6	24.4
R1225zc	220–370	0.94–9.42	3.6	17.4

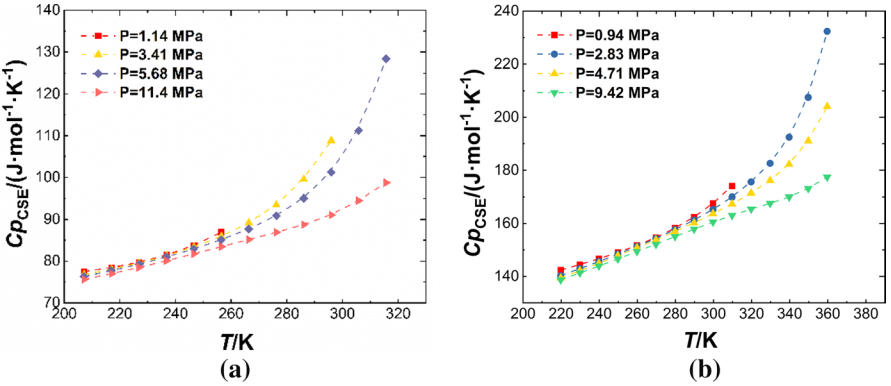

Fig. 4 Liquid heat capacity of *Class 3* refrigerants (R1141 (**a**) and R1225zc (**b**)) predicted by CSE

For Class 3 refrigerants, the comparison can only be performed between two general methods CSE and CEOS. The results are shown in Fig. 3 and Table 6. The AAD % and MAD % between CSE and CEOS were 6.6 % and 24.4 % for R1141, and 3.6 % and 17.4 % for R1225zc. As with class 1 and class 2 refrigerants, heat capacity values calculated from CEOS were bigger than those from CSE. The deviations became larger at higher temperatures, and a strong linear relation was also observed with Pearson factors of 0.9988 for R1141 and 0.9845 for R1225zc. Furthermore, the calculated points of CSE for R1141 and R1225zc are exhibited in Fig. 4 to show their variation trends versus temperature and pressure. The isobaric heat capacity would increase with the rise of temperature, and trended to be infinite near the critical point.

4 Discussion and Conclusions

In this paper, three different theoretical models were compared in liquid isobaric heat capacity prediction for hydrofluoroolefins refrigerants, which were general cubic EOS, specific fundamental EOSs, and a general corresponding state equation (CSE). To perform calculations for a certain object, CEOS and CSE need only several characteristic parameters (critical points and acentric factor), while FEOS needs at least volumetric experimental data (e.g., vapor pressure, saturated liquid density) to determine its specific structure and coefficients. Considering that isobaric heat capacity is a second-order derivative property, the accuracy of FEOS in this calculation highly relies on whether calorimetric property data were used in correlation.

Nine HFOs were selected for this study and were divided into 3 classes based on whether experimental c_p data and FEOS were available. The comparison showed that both CSE and FEOS represent available experimental data well with AADs % less than the reported experimental uncertainties. For refrigerants without experimental heat capacity, CSE and FEOS showed good agreements with all the AADs % less than 3.6 %.

The selected CEOS always provided relatively bigger predictions than experiments or the other two methods, and the deviations tended to be larger at higher temperatures. Despite that, calculated data of CEOS showed a strong linear relation with the others, which suggested that there might be a potential linear modification or correlation for CEOS in improving its heat capacity calculations. Finally, when there were no experimental data available, CSE used in this study could be a very useful and reliable preliminary evaluation tool for the liquid heat capacity of hydrofluoroolefins, considering its performance and easy application. It also indicated that for liquid isobaric heat capacity, the corresponding state principle works well within hydrofluoroolefins, and this conception could be possibly used in other thermophysical properties.

Appendix

Isobaric heat capacity data points calculated from cubic equation of state (CEOS) and corresponding state equation (CSE) are listed in the following Tables 7, 8, 9, 10, 11, and 12.

Table 7 Isobaric heat capacity of R1123 calculated from CEOS and CSE

T/K	*P*/MPa	Cp_{CEOS}(J·mol^{-1}·K^{-1})[a]	Cp_{CSE}(J·mol^{-1}·K^{-1})[b]	*T*/K	*P*/MPa	Cp_{CEOS}(J·mol^{-1}·K^{-1})	Cp_{CSE}(J·mol^{-1}·K^{-1})
210	1	94.4	101.0	210	5	93.1	99.7
220	1	97.2	102.0	220	5	95.6	101.2
230	1	100.3	103.3	230	5	98.3	102.8
240	1	104.0	105.2	240	5	101.3	104.7
250	1	108.4	107.8	250	5	104.7	106.8
260	1	113.8	111.4	260	5	108.7	109.2
210	2	94.0	100.6	270	5	113.4	112.1
220	2	96.7	101.8	280	5	119.1	115.7
230	2	99.8	103.2	290	5	126.5	120.5
240	2	103.3	105.1	300	5	136.7	127.6
250	2	107.3	107.5	310	5	152.4	139.1
260	2	112.3	110.7	320	5	182.0	159.0
270	2	118.6	114.9	210	10	91.8	98.9
280	2	127.1	120.8	220	10	94.0	100.3
290	2	140.2	129.3	230	10	96.3	101.9
210	3	93.7	100.2	240	10	98.8	103.6
220	3	96.3	101.5	250	10	101.5	105.4
230	3	99.3	103.1	260	10	104.5	107.3
240	3	102.6	105.0	270	10	107.9	109.2
250	3	106.4	107.3	280	10	111.6	111.1
260	3	110.9	110.2	290	10	115.8	113.2
270	3	116.6	113.8	300	10	120.6	115.8
280	3	124.0	118.7	310	10	126.3	119.8
290	3	134.4	125.7	320	10	132.9	124.7
300	3	151.6	136.4				

[a]Cp_{CEOS}: isobaric heat capacity calculated from cubic equation of state (PR); [b]Cp_{CSE}: isobaric heat capacity calculated from corresponding state equation

Table 8 Isobaric heat capacity of R1216 calculated from CEOS and CSE

T/K	P/MPa	Cp_{CEOS}(J·mol^{-1}·K^{-1})[a]	Cp_{CSE}(J·mol^{-1}·K^{-1})[b]	T/K	P/MPa	Cp_{CEOS}(J·mol^{-1}·K^{-1})	Cp_{CSE}(J·mol^{-1}·K^{-1})
210	1	143.9	153.8	320	3	207.3	199.4
220	1	147.6	156.0	330	3	224.2	212.5
230	1	151.6	158.3	340	3	254.1	233.9
240	1	155.8	160.8	210	5	142.7	150.6
250	1	160.3	163.7	220	5	146.2	153.5
260	1	165.2	167.1	230	5	149.8	156.5
270	1	170.7	171.1	240	5	153.6	159.5
280	1	177	176.0	250	5	157.5	162.6
290	1	184.5	182.1	260	5	161.7	165.8
300	1	194.1	190.1	270	5	166.1	169.2
210	2	143.5	152.4	280	5	170.9	172.8
220	2	147.3	155.0	290	5	176.1	176.4
230	2	151.1	157.6	300	5	181.9	180.3
240	2	155.2	160.4	310	5	188.5	184.7
250	2	159.5	163.5	320	5	196.4	190.1
260	2	164.2	166.9	330	5	206	197.6
270	2	169.4	170.7	340	5	218.4	208.6
280	2	175.2	175.0	350	5	235.6	221.8
290	2	181.9	180.2	210	10	141.4	150.1
300	2	190.1	186.5	220	10	144.7	152.6
310	2	200.7	194.8	230	10	148.1	155.2
320	2	216	206.4	240	10	151.5	157.9
330	2	242.4	224.2	250	10	155	160.8
210	3	143.2	151.6	260	10	158.6	163.7
220	3	146.9	154.3	270	10	162.3	166.7
230	3	150.7	157.2	280	10	166.1	169.6
240	3	154.6	160.1	290	10	170	172.3
250	3	158.8	163.2	300	10	174.2	174.8
260	3	163.3	166.6	310	10	178.5	177.0
270	3	168.2	170.2	320	10	183	179.2
280	3	173.6	174.2	330	10	187.8	181.9
290	3	179.7	178.7	340	10	192.8	186.3
300	3	186.8	184.0	350	10	198	203.3
310	3	195.7	190.6				

[a]Cp_{CEOS}: isobaric heat capacity calculated from cubic equation of state (PR); [b]Cp_{CSE}: isobaric heat capacity calculated from corresponding state equation

Table 9 Isobaric heat capacity of R1243zf calculated from CEOS and CSE

T/K	*P*/MPa	Cp_{CEOS}(J·mol^{-1}·K^{-1})[a]	Cp_{CSE}(J·mol^{-1}·K^{-1})[b]	*T*/K	*P*/MPa	Cp_{CEOS}(J·mol^{-1}·K^{-1})	Cp_{CSE}(J·mol^{-1}·K^{-1})
220	1	110.1	116.9	330	3	166.6	155.7
230	1	113.8	119.1	340	3	179.7	164.8
240	1	117.7	121.3	350	3	200.6	178.5
250	1	121.7	123.8	360	3	246.1	201.1
260	1	125.9	126.4	220	5	109	114.1
270	1	130.4	129.4	230	5	112.5	117.0
280	1	135.3	132.8	240	5	116.1	119.8
290	1	140.9	136.7	250	5	119.7	122.7
300	1	147.3	141.6	260	5	123.5	125.6
310	1	155.3	147.6	270	5	127.3	128.6
220	2	109.8	115.7	280	5	131.4	131.6
230	2	113.5	118.2	290	5	135.8	134.8
240	2	117.2	120.8	300	5	140.5	138.1
250	2	121.1	123.5	310	5	145.6	141.6
260	2	125.2	126.3	320	5	151.5	145.4
270	2	129.5	129.3	330	5	158.3	149.9
280	2	134.2	132.5	340	5	166.5	155.6
290	2	139.4	136.2	350	5	177	163.7
300	2	145.2	140.4	360	5	191.3	175.6
310	2	152.2	145.5	220	10	107.9	113.5
320	2	160.9	151.7	230	10	111.2	116.2
330	2	172.7	160.0	240	10	114.5	118.9
340	2	191.2	171.7	250	10	117.8	121.6
220	3	109.6	115.0	260	10	121.2	124.3
230	3	113.2	117.7	270	10	124.6	127.1
240	3	116.8	120.4	280	10	128.1	129.9
250	3	120.6	123.2	290	10	131.6	132.6
260	3	124.6	126.1	300	10	135.3	135.2
270	3	128.7	129.1	310	10	139.1	137.7
280	3	133.2	132.3	320	10	143.1	140.0
290	3	138	135.7	330	10	147.3	142.2
300	3	143.4	139.5	340	10	151.8	144.5
310	3	149.7	143.9	350	10	156.5	147.5
320	3	157.1	149.1	360	10	161.5	151.6

[a]Cp_{CEOS}: isobaric heat capacity calculated from cubic equation of state (PR); [b]Cp_{CSE}: isobaric heat capacity calculated from corresponding state equation

Table 10 Isobaric heat capacity of R1234ze(Z) calculated from CEOS and CSE

T/K	P/MPa	Cp_{CEOS}(J·mol^{-1}·K^{-1})[a]	Cp_{CSE}(J·mol^{-1}·K^{-1})[b]	T/K	P/MPa	Cp_{CEOS}(J·mol^{-1}·K^{-1})	Cp_{CSE}(J·mol^{-1}·K^{-1})
250	1	130.6	140.3	380	3	197.4	188.1
260	1	133.4	141.6	390	3	214.8	200.9
270	1	136.4	143.1	400	3	245.8	220.8
280	1	139.7	144.9	410	3	336.4	253.1
290	1	143.2	147.1	250	5	129.5	137.2
300	1	147.1	149.6	260	5	132.1	139.2
310	1	151.3	152.5	270	5	134.8	141.4
320	1	156	156.0	280	5	137.8	143.6
330	1	161.4	160.2	290	5	140.9	146.1
340	1	167.7	165.3	300	5	144.3	148.6
350	1	175.4	171.8	310	5	147.8	151.4
250	2	130.3	139.0	320	5	151.7	154.3
260	2	133	140.7	330	5	155.8	157.3
270	2	136	142.5	340	5	160.3	160.5
280	2	139.1	144.6	350	5	165.3	164.0
290	2	142.6	146.9	360	5	170.9	167.8
300	2	146.3	149.4	370	5	177.4	172.3
310	2	150.3	152.3	380	5	185.1	177.9
320	2	154.8	155.6	390	5	194.7	185.6
330	2	159.8	159.3	400	5	207.2	196.5
340	2	165.5	163.7	410	5	224.7	210.7
350	2	172.2	169.0	250	10	128.3	136.4
360	2	180.5	175.5	260	10	130.7	138.3
370	2	191.5	184.0	270	10	133.2	140.2
380	2	207.4	195.7	280	10	135.9	142.3
250	3	130	138.2	290	10	138.7	144.6
260	3	132.7	140.0	300	10	141.6	147.0
270	3	135.6	142.0	310	10	144.7	149.5
280	3	138.7	144.2	320	10	147.9	152.0
290	3	142	146.6	330	10	151.2	154.5
300	3	145.6	149.2	340	10	154.7	156.9
310	3	149.4	152.0	350	10	158.4	159.1
320	3	153.6	155.1	360	10	162.2	161.3
330	3	158.3	158.6	370	10	166.2	163.3
340	3	163.5	162.5	380	10	170.5	165.5
350	3	169.6	167.0	390	10	175	168.2
360	3	176.7	172.3	400	10	179.7	171.8
370	3	185.6	179.1	410	10	184.8	177.4

[a]Cp_{CEOS}: isobaric heat capacity calculated from cubic equation of state (PR); [b]Cp_{CSE}: isobaric heat capacity calculated from corresponding state equation

Table 11 Isobaric heat capacity of R1141 calculated from CEOS and CSE

T/K	*P*/MPa	Cp_{CEOS}(J·mol^{-1}·K^{-1})[a]	Cp_{CSE}(J·mol^{-1}·K^{-1})[b]	*T*/K	*P*/MPa	Cp_{CEOS}(J·mol^{-1}·K^{-1})	Cp_{CSE}(J·mol^{-1}·K^{-1})
207.2	1.1	75.0	77.5	256.5	4.5	89.8	85.5
217.0	1.1	77.7	78.4	266.3	4.5	94.8	88.4
226.9	1.1	80.8	79.7	276.2	4.5	101.0	92.1
236.7	1.1	84.4	81.4	286.1	4.5	109.4	97.1
246.6	1.1	88.6	83.8	295.9	4.5	121.9	104.6
256.5	1.1	93.9	87.0	305.8	4.5	144.3	117.2
207.2	2.3	74.6	77.1	207.2	5.7	73.7	76.3
217.0	2.3	77.3	78.2	217.0	5.7	76.1	77.7
226.9	2.3	80.2	79.6	226.9	5.7	78.7	79.3
236.7	2.3	83.6	81.4	236.7	5.7	81.7	81.0
246.6	2.3	87.6	83.6	246.6	5.7	85.0	82.9
256.5	2.3	92.4	86.4	256.5	5.7	88.8	85.1
266.3	2.3	98.5	90.1	266.3	5.7	93.3	87.7
276.2	2.3	106.9	95.3	276.2	5.7	98.8	90.9
286.1	2.3	119.8	102.7	286.1	5.7	105.9	95.1
207.2	3.4	74.3	76.8	295.9	5.7	115.7	101.2
217.0	3.4	76.9	78.0	305.8	5.7	130.9	111.2
226.9	3.4	79.7	79.5	315.7	5.7	159.7	128.4
236.7	3.4	82.9	81.3	207.2	11.4	72.4	75.6
246.6	3.4	86.6	83.4	217.0	11.4	74.5	77.0
256.5	3.4	91.0	85.9	226.9	11.4	76.7	78.5
266.3	3.4	96.5	89.2	236.7	11.4	79.2	80.1
276.2	3.4	103.7	93.5	246.6	11.4	81.8	81.8
286.1	3.4	113.9	99.5	256.5	11.4	84.6	83.5
295.9	3.4	130.8	108.8	266.3	11.4	87.8	85.2
207.2	4.5	74.0	76.5	276.2	11.4	91.3	86.9
217.0	4.5	76.5	77.9	286.1	11.4	95.3	88.7
226.9	4.5	79.2	79.4	295.9	11.4	99.9	91.1
236.7	4.5	82.3	81.1	305.8	11.4	105.2	94.5
246.6	4.5	85.8	83.1	315.7	11.4	111.4	98.7

[a]Cp_{CEOS}: isobaric heat capacity calculated from cubic equation of state (PR); [b]Cp_{CSE}: isobaric heat capacity calculated from corresponding state equation

Table 12 Isobaric heat capacity of R1225zc calculated from CEOS and CSE

T/K	P/MPa	Cp_{CEOS}(J·mol^{-1}·K^{-1})[a]	Cp_{CSE}(J·mol^{-1}·K^{-1})[b]	T/K	P/MPa	Cp_{CEOS}(J·mol^{-1}·K^{-1})	Cp_{CSE}(J·mol^{-1}·K^{-1})
219.8	0.9	134	142.4	329.7	2.8	191.3	182.6
229.8	0.9	137.6	144.5	339.7	2.8	204.8	192.5
239.8	0.9	141.4	146.7	349.7	2.8	226.4	207.5
249.8	0.9	145.4	149.0	359.7	2.8	272.9	232.4
259.8	0.9	149.6	151.7	219.8	4.7	132.9	139.4
269.8	0.9	154.1	154.7	229.8	4.7	136.3	142.2
279.8	0.9	159.1	158.3	239.8	4.7	139.8	145.0
289.7	0.9	164.8	162.4	249.8	4.7	143.4	147.8
299.7	0.9	171.4	167.6	259.8	4.7	147.2	150.8
309.7	0.9	179.5	174.0	269.8	4.7	151.1	153.8
219.8	1.9	133.7	141.1	279.8	4.7	155.3	157.0
229.8	1.9	137.2	143.6	289.7	4.7	159.7	160.2
239.8	1.9	141	146.1	299.7	4.7	164.5	163.7
249.8	1.9	144.8	148.7	309.7	4.7	169.9	167.3
259.8	1.9	148.9	151.5	319.7	4.7	175.9	171.4
269.8	1.9	153.3	154.5	329.7	4.7	183	176.1
279.8	1.9	158	158.0	339.7	4.7	191.6	182.3
289.7	1.9	163.3	161.8	349.7	4.7	202.6	191.1
299.7	1.9	169.3	166.3	359.7	4.7	217.6	204.1
309.7	1.9	176.4	171.7	219.8	9.4	131.8	138.7
319.7	1.9	185.4	178.5	229.8	9.4	135	141.3
329.7	1.9	197.4	187.4	239.8	9.4	138.2	143.9
339.7	1.9	216.1	200.2	249.8	9.4	141.5	146.6
219.8	2.8	133.4	140.3	259.8	9.4	144.9	149.4
229.8	2.8	136.9	143.0	269.8	9.4	148.4	152.1
239.8	2.8	140.6	145.6	279.8	9.4	151.9	155.1
249.8	2.8	144.3	148.4	289.7	9.4	155.6	157.8
259.8	2.8	148.3	151.3	299.7	9.4	159.3	160.5
269.8	2.8	152.5	154.3	309.7	9.4	163.3	163.1
279.8	2.8	157	157.7	319.7	9.4	167.4	165.5
289.7	2.8	162	161.3	329.7	9.4	171.8	167.6
299.7	2.8	167.5	165.3	339.7	9.4	176.4	170.0
309.7	2.8	173.9	169.9	349.7	9.4	181.3	173.1
319.7	2.8	181.6	175.6	359.7	9.4	186.5	177.4

[a]Cp_{CEOS}: isobaric heat capacity calculated from cubic equation of state (PR); [b]Cp_{CSE}: isobaric heat capacity calculated from corresponding state equation

Acknowledgments This work is financially supported by the National Natural Science Foundation of China (No. 51906216).

Declarations

Conflict of interest The authors declare that they have no known competing financial interests or personal relationships that could have appeared to influence the work reported in this paper.

References

1. The European Parliament and the Council of the European Union. Regulation (EC) No 842/2006 of the European Parliament and of the Council of 17 May 2006 on certain fluorinated greenhouse gases (OJ L 161, 14.6.2006, p. 1). 2006.
2. The European Parliament and the Council of the European Union. Regulation (EU) No 517/2014 of the European Parliament and of the Council of 16 April 2014 on fluorinated greenhouse gases and repealing Regulation (EC) No 842/2006 (OJ L 150/195, 20.5.2014, p. 1). 2014.
3. UNEP. The Kigali Amendment to the Montreal Protocol: HFC Phase-down. Kigali, 2016.
4. X. Wang, Y. Yan, B. Li, X. Hao, N. Gao, G. Chen, Prospect of solar-driven ejector-compression hybrid refrigeration system with low GWP refrigerants in summer of Guangzhou and Beijing. Int. J. Refrig. **117**, 230–236 (2020)
5. IPCC. Climate Change 2014: Synthesis Report. Contribution of Working Groups I, II and III to the Fifth Assessment Report of the Intergovernmental Panel on Climate Change. Geneva, Switzerland, 2014.
6. X. Wang, Y. Li, Y. Yan, E. Wright, N. Gao, G. Chen, Prediction on the viscosity and thermal conductivity of hfc/hfo refrigerants with artificial neural network models. Int. J. Refrig. **119**, 316–325 (2020)
7. M.O. McLinden, J.S. Brown, R. Brignoli, A.F. Kazakov, P.A. Domanski, Limited options for low-global-warming-potential refrigerants. Nat. Commun. **8**, 14476 (2017)
8. S. Bobbo, G. Di Nicola, C. Zilio, J.S. Brown, L. Fedele, Low GWP halocarbon refrigerants: a review of thermophysical properties. Int. J. Refrig. **90**, 181–201 (2018)
9. Y. Zheng, H. Gao, Q. Chen, X. Meng, J. Wu, Isobaric heat capacity measurements of liquid HFE-7200 and HFE-7500 from 245 to 353 K at pressures up to 15 MPa. Fluid Phase Equilib. **372**, 56–62 (2014)
10. N. Gao, Y. Jiang, J. Wu, Y. He, G. Chen, Measurements of the isobaric heat capacity of R1234yf in liquid phase at temperatures from 305 K to 355 K and pressures up to 5 MPa. Fluid Phase Equilib. **376**, 64–68 (2014)
11. K. Tanaka, G. Takahashi, Y. Higashi, Measurements of the isobaric specific heat capacities for trans-1,3,3,3-tetrafluoropropene (HFO-1234ze(E)) in the liquid phase. J. Chem. Eng. Data **55**, 2267–2270 (2010)
12. Hulse R, Singh R, Pham H. Physical Properties of HFO-1234yf. In: Proceedings of the Third IIR International Conference on Thermophysical Properties and Transfer Processes of Refrigerants. 2009, Boulder, Colorado.
13. Y. Kano, Y. Kayukawa, K. Fujii, H. Sato, Ideal-gas heat capacity for 2,3,3,3-Tetrafluoropropene (HFO-1234yf) determined from speed-of-sound measurements. Int. J. Thermophys. **31**, 2051–2058 (2010)
14. R.A. Marriott, M.A. White, Comparison of ab initio and group additive ideal gas heat capacities. AIChE J. **51**, 292–297 (2005)

15. D. Peng, D.B. Robinson, A new two-constant equation of state. Ind. Eng. Chem. Fundam. **15**, 59–64 (1976)
16. R. Schmidt, W. Wagner, A new form of the equation of state for pure substances and its application to oxygen. Fluid Phase Equilib. **19**(3), 175–200 (1985)
17. W.A. Fouad, L.F. Vega, Next generation of low global warming potential refrigerants: thermodynamic properties molecular modeling. AIChE J. **64**(1), 250–262 (2018)
18. K. Kang, X. Wang, G. Kontogeorgis, X. Liang, Modeling hydrofluoroolefins with the cubic plus association and perturbed-chain statistical associationg fluid theory equations of state. Ind. Eng. Chem. Res. **57**, 17289–17300 (2018)
19. G. Raabe, E.J. Maginn, Molecular modeling of the vapor liquid equilibrium properties of the alternative refrigerant 2,3,3,3-tetrafluoro-1-propene (HFO-1234yf). J. Phys. Chem. Lett. **1**(1), 93–96 (2010)
20. G. Raabe, E.J. Maginn, A force field for 3,3,3-fluoro-1-propenes, including HFO-1234yf. J. Phys. Chem. B **114**(31), 10133–10142 (2010)
21. G. Raabe, Molecular modeling of fluoropropene refrigerants. J. Phys. Chem. B **116**(19), 5744–5751 (2012)
22. T.J. Lyman, R.P. Danner, Correlation of liquid heat capacities with a four-parameter corresponding states method. AIChE J. **22**(4), 759–765 (1976)
23. N. Gao, X. Wang, Y. Xuan, G. Chen, An artificial neural network for the residual isobaric heat capacity of liquid HFC and HFO refrigerants. Int. J. Refrig. **98**, 381–387 (2019)
24. N. Gao, G. Chen, L. Tang, A corresponding state equation for the prediction of isobaric heat capacity of liquid HFC and HFO refrigerants. Fluid Phase Equilib. **456**, 1–6 (2018)
25. N. Gao, G. Chen, R. Li, Y. Wang, Y. He, B. Yang, Measurements of the isobaric heat capacity of pressurized liquid trans-1,3,3,3-tetrafluoropropene [R1234ze(E)] by scanning calorimetry. J. Therm. Anal. Calorim. **122**(3), 1469–1476 (2015)
26. K. Tanaka, Y. Higashi, R. Akasaka, Measurements of the Isobaric Specific Heat Capacity and Density for HFO-1234yf in the Liquid Phase. J. Chem. Eng. Data **55**, 901–903 (2010)
27. M. Richter, M.O. McLinden, E.W. Lemmon, Thermodynamic properties of 2,3,3,3-tetrafluoroprop-1-ene (R1234yf): vapor pressure and p-rho-T measurements and an equation of state. J. Chem. Eng. Data **56**, 3254–3264 (2011)
28. McLinden M O, Thol M, Lemmon E W. Thermodynamic Properties of Trans-1,3,3,3-tetrafluoropropene [R1234ze(E)]: Measurements of Density and Vapor Pressure and a Comprehensive Equation of State. International Refrigeration and Air Conditioning Conference, 2010, Purdue.
29. R. Akasaka, Y. Higashi, N. Sakoda, S. Fukuda, E.W. Lemmon, Thermodynamic properties of trifluoroethene (R1123): (p, rho, T) behavior and fundamental equation of state. Int. J. Refrig. **119**, 457–467 (2020)
30. Lemmon E W, Bell I H, Huber M L, et al. NIST Standard Reference Database 23, DLL Version Number 10.0, 2018.
31. R. Akasaka, E.W. Lemmon, Fundamental equations of state for cis-1,3,3,3-Tetrafluoropropene [R11234ze(Z)] and 3,3,3-trifluoropropene (R-1243zf). J. Chem. Eng. Data **64**, 4679–4691 (2019)
32. K.G. Joback, R.C. Reid, Estimation of pure-component properties from group contributions. Chem. Eng. Commun. **57**, 233–243 (1987)

Authors and Affiliations

Neng Gao[1,4] · Likai Zhou[2] · Xuehui Wang[3] · Guangming Chen[1,2]

[1] NingboTech University, Ningbo 315100, China

[2] Zhejiang University, Hangzhou 310027, China

[3] Department of Chemical Engineering, Imperial College London, London SW7 2AZ, UK

[4] Zhejiang Engineering Research Center for Intelligent Marine Ranch Equipment, Ningbo 315100, China